

 Open access • Journal Article • DOI:10.1021/NL070900E

Imaging of the Schottky barriers and charge depletion in carbon nanotube transistors.

— [Source link](#) 

Marcus Freitag, [James C. Tsang](#), [Ageeth A. Bol](#), [Dongning Yuan](#) ...+2 more authors

Institutions: [IBM](#), [Duke University](#)

Published on: 09 Jun 2007 - [Nano Letters](#) (American Chemical Society)

Topics: [Schottky barrier](#), [Surface photovoltage](#), [Carbon nanotube field-effect transistor](#), [Nanotube](#) and [Schottky diode](#)

Related papers:

- [Scanning Photocurrent Imaging and Electronic Band Studies in Silicon Nanowire Field Effect Transistors](#)
- [Photocurrent Imaging of Charge Transport Barriers in Carbon Nanotube Devices](#)
- [Photoelectronic transport imaging of individual semiconducting carbon nanotubes](#)
- [Photocurrent Imaging of p-n Junctions and Local Defects in Ambipolar Carbon Nanotube Transistors](#)
- [Photoconductivity of Single Carbon Nanotubes](#)

Share this paper:    

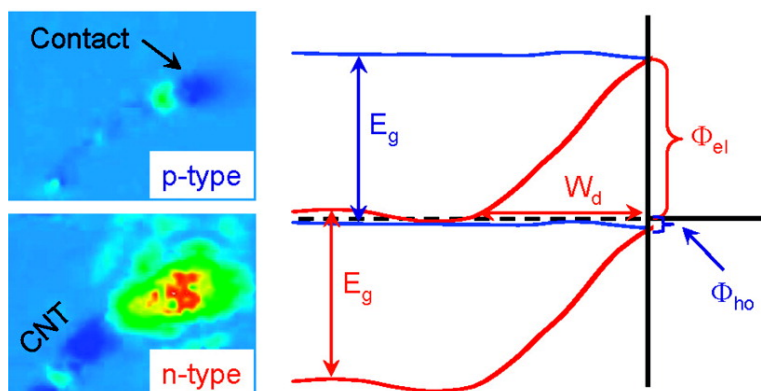
View more about this paper here: <https://typeset.io/papers/imaging-of-the-schottky-barriers-and-charge-depletion-in-47vm2rppko>

Imaging of the Schottky Barriers and Charge Depletion in Carbon Nanotube Transistors

Marcus Freitag, James C. Tsang, Ageeth Bol, Dongning Yuan, Jie Liu, and Phaedon Avouris

Nano Lett., 2007, 7 (7), 2037-2042 • DOI: 10.1021/nl070900e

Downloaded from <http://pubs.acs.org> on January 1, 2009



More About This Article

Additional resources and features associated with this article are available within the HTML version:

- Supporting Information
- Links to the 2 articles that cite this article, as of the time of this article download
- Access to high resolution figures
- Links to articles and content related to this article
- Copyright permission to reproduce figures and/or text from this article

[View the Full Text HTML](#)

Imaging of the Schottky Barriers and Charge Depletion in Carbon Nanotube Transistors

Marcus Freitag,^{*,†} James C. Tsang,[†] Ageeth Bol,[†] Dongning Yuan,[‡] Jie Liu,[‡] and Phaedon Avouris[†]

IBM T. J. Watson Research Center, 1101 Kitchawan Road, Yorktown Heights, New York 10598, and Department of Chemistry, Duke University, Durham, North Carolina 27708

Received April 17, 2007; Revised Manuscript Received May 24, 2007

ABSTRACT

The photovoltage produced by local illumination at the Schottky contacts of carbon nanotube field-effect transistors varies substantially with gate voltage. This is particularly pronounced in ambipolar nanotube transistors where the photovoltage switches sign as the device changes from p-type to n-type. The detailed transition through the insulating state can be recorded by mapping the open-circuit photovoltage as a function of excitation position. These photovoltage images show that the band-bending length can grow to many microns when the device is depleted. In our palladium-contacted devices, the Schottky barrier for electrons is much higher than that for holes, explaining the higher p-type current in the transistor. The depletion width is 1.5 μm near the n-type threshold and smaller than our resolution of 400 nm near the p-type threshold. Internal photoemission from the metal contact to the carbon nanotube and thermally assisted tunneling through the Schottky barrier are observed in addition to the photocurrent that is generated inside the carbon nanotube.

Semiconducting single-walled carbon nanotubes (CNTs) can act as nanoscale switching elements when incorporated between two metal contacts and a nearby third electrode is used to gate them.^{1,2} Even though the geometry of the carbon nanotube field-effect transistor (CNTFET) is reminiscent of the well-known metal-oxide semiconductor field-effect transistor (MOSFET), its switching action is distinct. In a MOSFET, the charge density in the semiconducting channel is modulated by the gate, whereas, in a CNTFET, the transmission through Schottky barriers³ formed at the metal source/drain-CNT contacts is modulated as well.^{4,5} By a proper choice of contact metal, the Schottky-barrier height for one type of carrier (electron or hole) can be minimized,⁶ or alternatively, the Fermi-level lineup between the metal and the nanotube can be adjusted near midgap, resulting in ambipolar CNTFETs.⁷ Not only the height but also the width of the barrier determines the performance of the CNTFET since injection of carriers into the CNT channel involves primarily tunneling through the Schottky barrier.

Two methods have been reported that can be used to directly observe the Schottky barriers in active devices. One is scanned gate microscopy where a conductive tip is used to gate the nanotube locally.⁵ The other is photocurrent microscopy where images of the photocurrent are generated

when a laser spot is focused to subdevice dimensions and scanned across the device.⁸ In both of the published experiments, the CNTFETs were unipolar, and only the Schottky barrier for holes could be studied. Here we report laser-scanning short-circuit photocurrent and open-circuit photovoltage images of p-type and ambipolar CNTFETs. We detect carriers that are photogenerated in the CNT and separated by the built-in field of the Schottky barrier. We also observe internal photoemission/thermal injection from the metal contact through the Schottky barrier into the nanotube. In ambipolar CNTs, we can image the switching action of the Schottky barrier. While the short-circuit photocurrent diminishes in the “off” transistor state, the open-circuit photovoltage is maximized under these conditions. This allows us to measure the depletion layer width, which extends less than 400 nm at the p-type threshold, expands to many micrometers in the transistor off state, and becomes 1.5 micrometers at the n-type threshold.

Single-walled CNTs are grown in two different chemical vapor deposition (CVD) systems directly on silicon substrates with 100–200 nm of silicon oxide. One process, based on ethanol CVD, produces $\sim 10 \mu\text{m}$ long CNTs with diameters between 1 and 2 nm. The recipe is similar to the one in ref 9 with the exception that 3–4 nm iron oxide nanoparticles are used as the catalyst instead of CoMo-doped porous silica. The other process is based on CH_4 (1500 sccm), C_2H_4 (30

* Corresponding author. E-mail: mfreitag@us.ibm.com.

[†] IBM T. J. Watson Research Center.

[‡] Duke University.

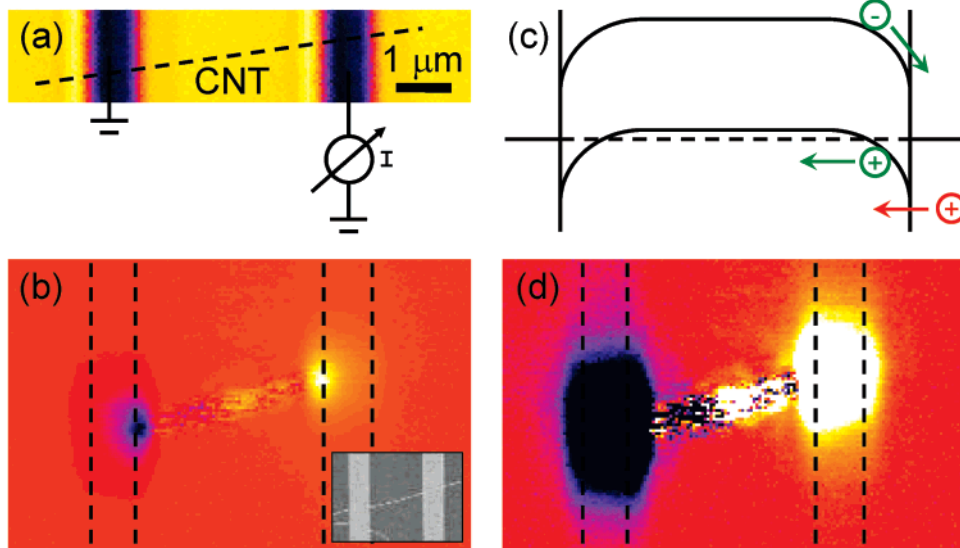


Figure 1. Short-circuit photocurrent imaging of a p-type CNTFET. (a) Reflected light image in a laser-scanning microscope showing the two contacts of a CNTFET. The CNT and the measurement setup for the photocurrent measurements are indicated. (b) Short-circuit photocurrent image of this device under $500 \mu\text{W}$ of $\lambda = 457.9 \text{ nm}$ laser excitation focused into an $\sim 400 \text{ nm}$ spot. Yellow areas correspond to a positive I_{SC} , purple areas represent a negative I_{SC} . The color scale spans $\pm 15 \text{ nA}$. The outlines of the contacts are indicated. (c) Schematic of the band bending in the p-type device. “Green” carriers refer to a photocurrent generated within the CNT, and “red” carriers refer to internal photoemission and thermally assisted tunneling processes. (d) The data from panel b displayed with a narrower color scale of $\pm 1 \text{ nA}$. Black and white areas are saturated. Inset: SEM image of the CNTFET.

sccm), and H_2 (750 sccm), uses Fe/Mo nanoparticles, and produces many hundreds of micrometers-long CNTs with diameters around 2–3 nm.¹⁰ CNTFET devices are fabricated by an e-beam lithography/30 nm palladium metallization/lift-off process. A thin $\sim 7 \text{ \AA}$ titanium layer improves the adhesion of the palladium. Measurements are done under an optical microscope with a $100 \times 0.8 \text{ NA}$ objective and Argon laser lines of 514.5 nm and 457.9 nm, producing a focus around 400 nm. The excitation is generally not in resonance with the CNTs and is chosen at short wavelengths to enhance lateral resolution. Typical powers on the sample are around $500 \mu\text{W}$, and no substantial heating of the CNT is observed. The sample is scanned on a piezoelectric stage with nanometer precision. Images generated by the back-reflected light are used to locate the contacts on our devices. For measurements of the open-circuit photovoltage, one contact is grounded and serves as the reference for the voltage measurement at the other contact. For short-circuit photocurrent measurements, one contact is grounded and the other contact is connected to a current preamplifier.

CNTFETs have been shown to produce a photocurrent when biased and illuminated with above-band gap light.^{11,12} Under illumination of the entire device, they do not usually show a photovoltage due to the existence of a mirror plane symmetry with respect to a plane perpendicular to the nanotube.¹³ However, in devices with two nonequivalent Schottky barriers, this symmetry is broken, and a photovoltage of up to 300 mV (i.e., a substantial fraction of the nanotube band gap) can be generated.¹⁴ The devices show rectifying transport characteristics in the dark, presumably dominated by one of the two Schottky barriers. Photovoltaic devices can be characterized by an open-circuit photovoltage V_{OC} , a short-circuit photocurrent I_{SC} , and a fill factor FF,

which measures the fraction of power that can be generated compared to the ideal case $V_{\text{OC}} \cdot I_{\text{SC}}$. Typical values for our asymmetric devices for incident power densities on the order of 100 KW/cm^2 are $V_{\text{OC}} \sim 100 \text{ mV}$, $I_{\text{SC}} \sim 100 \text{ pA}$, and $\text{FF} \sim 0.3$.

The mirror plane symmetry of a CNTFET can also be broken by focusing the excitation spot to subdevice dimensions so that only a small part of the nanotube is illuminated at a time. In the presence of potential modulations along the CNT, the photovoltage is a measure of the local potential gradient in the excitation region, which separates the photogenerated electrons and holes.¹⁵ By scanning the laser spot across the sample and assembling images of the photocurrent in a computer, we obtain a sensitive microscopic probe for local electronic transport parameters of CNTs. A photocurrent image of a semiconducting CNTFET under external bias has been reported before.⁸ The same group has also shown unbiased photocurrent images of metallic CNTs with depletion layers at the contacts.¹⁶ For the CNTFET, only one of the Schottky barriers was observed, and it was suggested that this device might have had dissimilar Schottky barriers.⁸ However, the bias voltage produces an asymmetry, which complicates the interpretation of the photocurrent data significantly.¹⁵ We therefore measured the *short-circuit* photocurrent I_{SC} or open-circuit photovoltage V_{OC} in about 20 different CNTFETs, and all of them exhibit a response at both Schottky barriers.

Figure 1 shows a representative measurement where I_{SC} was measured with a current preamplifier at the right contact, and a $\lambda = 457.9 \text{ nm}$ argon laser line was focused to an $\sim 400 \text{ nm}$ diameter spot and scanned across the sample. This device was p-type, and purple/yellow in Figure 1b corresponds to a negative/positive sign of I_{SC} . The Schottky barriers always

Figure 2. Short-circuit photocurrent and open-circuit photovoltage of an ambipolar CNTFET. (a) I_{SC} image of a 50 μm long CNTFET showing defect-related photocurrent generation in addition to the Schottky-barrier-related generation. The data in panels d–f are acquired in the indicated square. (b) Schematic of the band structure for p-type and n-type gating conditions. (c) Gate-voltage characteristic of the device. The sweep direction is indicated. (d,e) I_{SC} images of the contact region under various gate voltages. The sweep direction of the gate voltage (indicated by arrows) was reversed between the two sequences. Color scale: ± 2 nA. The laser power was ~ 800 μW , and the maximum photocurrent was ~ 5 nA. (f) Images of V_{OC} for the same region with gate voltages -10 , -5 , 0 , $+5$, and $+10$ V in this order. Color scale: ± 30 mV.

appear in *pairs of opposite sign*. Importantly, the arrangement of positive and negative regions at the contacts can be explained by the p-type character of our devices in the on state (Figure 1c), where photogenerated electrons should drift to the nearby metal electrode and holes toward the bulk of the nanotube. The magnitude of the photocurrent for excitation at the Schottky barriers was 15 nA for an excitation power of 500 μW . In addition to the strong and reproducible response from the Schottky barriers, there is a weak and noisy response from the body of the CNT, which can be attributed to changes in the environment that are induced by the laser light.¹⁷

Figure 1d shows the data from Figure 1b with a higher contrast. Black and white areas are now saturated. One can clearly see the edges of the metal contacts in the photocurrent images. Electrons that are excited in the metal and that travel to the junction without losing too much energy can overcome the barrier to the CNT and contribute to the photocurrent. In addition to this internal photoemission, which should only be significant for excitation very close to the interface, a temperature increase of the electrode will also help carriers tunnel through the Schottky barrier. We find that internal photoemission/thermally assisted tunneling at the metal contact is independent of the incident polarization. In contrast, when light is directly focused onto the Schottky barrier, polarization anisotropies around 2:1 are typically found, with the higher photocurrent recorded for polarization along the nanotube axis. The weaker than previously reported¹¹ polarization anisotropy for direct

excitation of the nanotube can be partially explained by the higher photon energy used (2.7 eV instead of 1.5 eV) and the larger diameters of the CNTs that were studied (~ 2 nm compared to 1.3 nm). Previously, the excitation was resonant with the E_{22} exciton,¹¹ while here we are exciting high in the fourth or fifth subband, where the overlap with the tail of the polarization-independent π -plasmon resonance becomes substantial.²⁴

Figure 2 shows photocurrent images of a different device, whose electronic characteristic was ambipolar and which was much longer (50 μm source–drain distance) than the device in Figure 1. When nanotubes are that long, it is common that the body of the CNT produces sizable local photovoltages, as seen in the additional spots along the CNT in Figure 2a. Defects can modulate the potential in a CNT, and, when the light is focused to a spot on the order of or smaller than typical defect separations, a photovoltage is produced.^{16,17} We focus here on the Schottky barrier region, which is responsible for the ambipolar characteristic of the CNT. As the backgate voltage is swept between -10 V and 10 V, the transistor undergoes a transition from p-type to insulating and finally to n-type (Figure 2c). During the sweep in opposite direction, the CNTFET experiences some hysteresis,^{18,19} but otherwise retraces its path from n-type through insulating to p-type.

A sequence of short-circuit photocurrent images of the right contact region is shown in Figure 2d,e. Similar sequences can be produced from the other contact. During the sweep from $+10$ V to -10 V (Figure 2d), the photocurrent

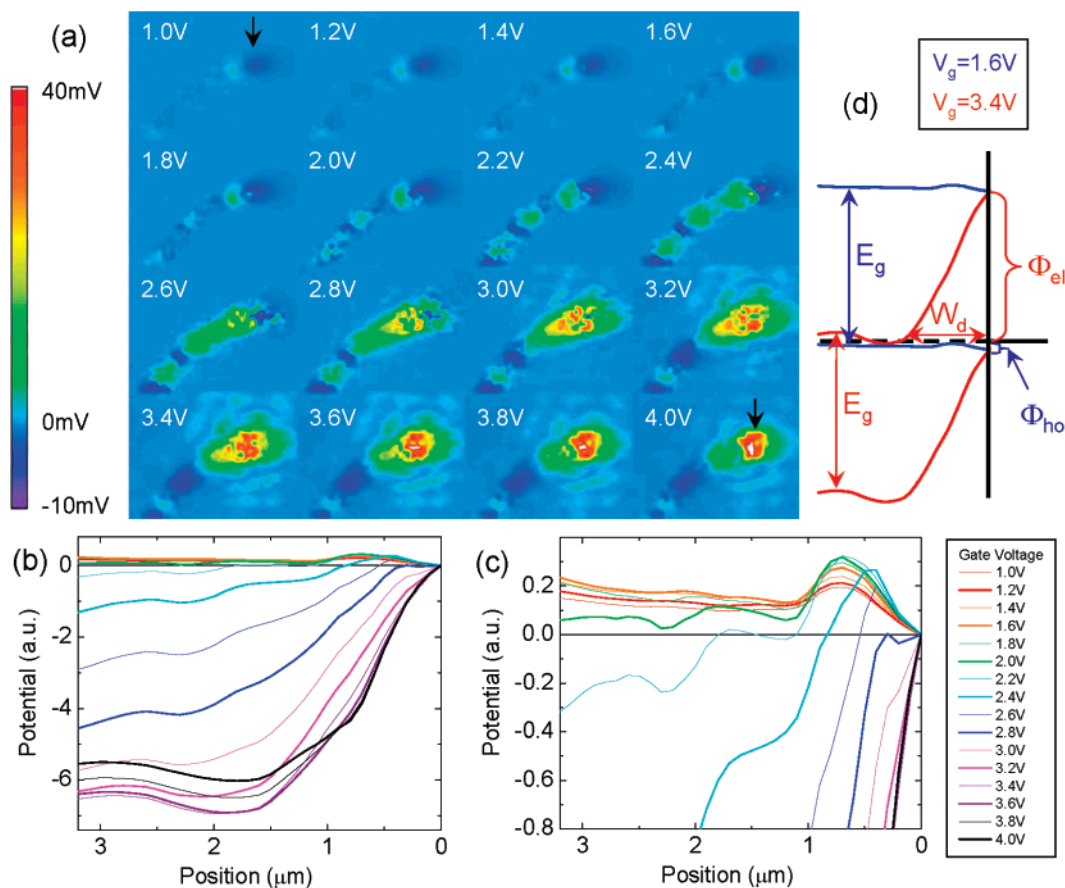


Figure 3. Open-circuit photovoltage microscopy of the contact region. (a) V_{OC} images of the Schottky-barrier region during the transition from p-type to n-type conduction in the transistor off state. Gate voltages are as indicated. The arrows point to the Schottky-barrier-related signal. Laser power was $900 \mu\text{W}$. A movie of the sequence is available as Supporting Information. (b) Integrated V_{OC} signal along the length of the CNT. The metal contact is located at the origin of the position scale, and the potential was fixed there for all gate voltages. Most of the movement in the bands happens between $V_G = 1.6$ and 3.4 V, where the CNT is depleted. (c) Plot b with a different y scale. (d) Schematic of the band bending for the two threshold voltages for hole and electron conduction at $V_G = 1.6$ and 3.4 V. Actual curves from panel b are used that indicate the band edges. The band gap is adjusted so that the Fermi level overlaps with the valance band at $V_G = 1.6$ V and the conduction band at $V_G = 3.4$ V.

from the Schottky barrier is negative (black contrast), then vanishes in the gap, and then reappears with opposite sign. On the reverse sweep from -10V to $+10\text{V}$ (Figure 2e), the Schottky barrier-related photocurrent flips sign again, and the hysteresis in the $I-V_G$ characteristics (Figure 2c) is reproduced in the I_{SC} images. Figure 2b depicts the situation schematically as the band bending changes from p-type to n-type when the gate voltage is swept. It is interesting to note that there exists a peak in the $I_{SC}(V_G)$ relationship (brightest spot in the sequence) of $I_{SC} \sim 5$ nA in the p-type on state around -2 V in Figure 2d and -4 V in Figure 2e. Resistance changes of the CNT should be mirrored in the short-circuit photocurrent, but this cannot explain the fact that the signal near the contact diminishes gradually at large negative gate voltages. The depletion width, however, can be expected to become very thin in the transistor on state, i.e., thinner than the laser spot size. The reduced active area will more than offset the higher collection efficiency due to increased interface fields present at more negative gate voltages.

While images of the short-circuit photocurrent can uniquely identify the n-type and p-type states of the ambipolar

Schottky-barrier transistor, the signal vanishes in the insulating state because of the high internal resistance of the nanotube channel. However, we find that the open-circuit photovoltage has complementary properties. It exhibits the highest signal in the off state (Figure 2f).²⁰ The open-circuit photovoltage can therefore show details of the transition between electron and hole conduction during the depleted state, where the CNT bands become very flat. It is important to note that the contrast of the features in the V_{OC} images is inverted compared to the that in I_{SC} images because a positive (negative) sign of the photovoltage corresponds to a negative (positive) photocurrent measured at the same electrode.

Figure 3a shows a sequence of open-circuit photovoltage images taken with small (0.2 V) steps in gate voltage. At $V_G = 1.0$ V, the nanotube is a hole conductor, and a narrow Schottky barrier is present (round blue spot marked by an arrow), whose width is smaller than our optical resolution of ~ 400 nm. At 2.6 V, there is still a p-type Schottky barrier at the contact, while a larger nanotube segment to the left of the contact starts to bend down (yellow area). At 3.2 V, the immediate contact region has finally switched as well, and an entire $2 \mu\text{m}$ -long nanotube segment starting at the contact

exhibits a uniform n-type band bending. The potential gradient due to the Schottky barrier for electrons thus extends far into the interior of the CNT. At even higher gate-voltage values, the depletion width gradually shrinks. The highest photovoltages of $V_{OC} = 40$ mV were measured in the n-type state. It is interesting that the contact region switches a few hundred millivolts in gate voltage after the area next to it. This might have to do with an additional interface dipole layer producing a potential with different range. Possible origins for such interface dipoles are adsorbents on the CNT/metal interface or charges in the oxide. For example, a gold/CNT interface has been found to exhibit a surface dipole if the interface is exposed to oxygen.²¹

Since the generated photovoltage is proportional to the potential gradient at the laser spot position, we can extract the band bending (Figure 3b,c) in the contact region from the data in Figure 3a.¹⁵ Line scans along the CNT were integrated for this purpose, and the potential at the physical position of the contact was set to zero. The transition from n-type to p-type band bending is evident in the figures. The movement of the bands stops when the Fermi level reaches the valence/conduction bands. This happens at threshold voltages of 1.6 V and 3.4 V, respectively. The difference (1.8 V) is about 4 times larger than the expected nanotube band gap, suggesting a gate efficiency factor of $\alpha \sim 0.25$, which is defined as $\Delta E_F = \alpha e \Delta V_G$, where ΔE_F and ΔV_G are changes in the Fermi level and gate voltage, respectively.²² V_G can be partially screened in the oxide and by the grounded contacts. In this gate-voltage range, the CNT is depleted, so no screening from the CNT is expected.

For gate voltages that are larger than 3.4 V or smaller than 1.6 V, the movement of the bands reverses slightly. This is probably an artifact of the technique. We are using a 400 nm wide spot to probe the device. If the band bending at the Schottky barrier gets very steep, as is presumably the case for heavy electrostatic doping, the generated photovoltage will stop increasing because less and less of the laser spot is contributing to the signal. In the integrated plots, this limits the slope of the bands close to the contacts, and thus it appears that the bands do not bend as far. In Figure 3c, we plot the data from Figure 3b in a different scale. The same reversal of the band movement happens for the p-type case. The hump in the curves in Figure 3c at around 300–700 nm is due to the previously discussed surface dipole at the contact.

In Figure 3d, the band profiles corresponding to the two threshold voltages are used to sketch both conduction and valence bands. The band gap is chosen so that the valence band at $V_G = 1.6$ V overlaps with the conduction band at $V_G = 3.4$ V. This is justified because, at the two threshold voltages, the valence (conduction) bands should line up with the Fermi level, which is fixed at zero bias. The ratio of Schottky barrier heights for electrons Φ_{el} and holes Φ_{ho} does not depend on the gate efficiency factor α and can be estimated from the figure. We find $\Phi_{el}/\Phi_{ho} \gg 1$, consistent with the better p-type conduction in Pd-contacted CNTs used in this study.⁶ There is an uncertainty in the exact position of the Fermi level, so we cannot quantify the small Schottky

barrier height for holes. It is clear, however, that the Schottky barrier height for electrons spans almost the entire nanotube band gap.

In addition to the Schottky barrier height, we can quantify the depletion width W_D at the various gate voltages. At the threshold for hole conduction ($V_G = 1.6$ V), we measure $W_D \sim 500$ nm, which is likely limited by the laser spot size rather than the true depletion width. However, in the off state, we find that the depletion width grows to many micrometers, as is evident from the slowly curving bands around $V_G = 2.8$ V. At the threshold for electron conduction, $W_D = 1.5 \mu\text{m}$.

The technique that we used to extract the potentials in a CNT should be valid as long as band bending happens over length scales that are large compared to the excitation spot size. We find that in our one-dimensional CNTFETs, this is the case over a substantial gate-voltage range that includes the transistor “off”-state and the threshold voltage for electron conduction, consistent with theoretical predictions of an extremely slowly decaying potential tail at interfaces in one dimension.³ In the future, we plan to perform measurements on CNTs with near-field excitation to probe the potential profile in the near-field region of the contact,²³ where the band bending could have a different functional form.

In conclusion, we have shown that the photovoltage produced in CNTFETs by local optical excitation can be used to characterize the Schottky barriers. There are two effects that lead to a photovoltage at the contacts: photons absorbed in the CNT produce electron–hole pairs that are separated by the built-in electric fields, and photons absorbed in the metal contact contribute through internal photoemission and thermally assisted tunneling. The short-circuit photocurrent and open-circuit photovoltage complement each other in gate-voltage-dependent measurements where the internal resistance of the CNTFET can span 3–6 orders of magnitude. We show that the Schottky barriers switch sign in ambipolar transistors, and that band bending can extend microns in the depleted transistor state.

Supporting Information Available: Movie of the transition from p-type to n-type conduction in the Schottky-barrier region in the transistor off state. This material is available free of charge via the Internet at <http://pubs.acs.org>.

References

- (1) Avouris, Ph. Electronics with Carbon Nanotubes. *Phys. World* **2007**, 20, 40.
- (2) Freitag, M. Carbon Nanotube Electronics and Devices. In *Carbon Nanotubes: Properties and Applications*; O’Connell, M. J., Ed.; CRC/Taylor & Francis: Boca Raton, FL, 2006; pp 83–117.
- (3) Léonard, F.; Tersoff, J. *Phys. Rev. Lett.* **1999**, 83, 5174.
- (4) Heinze, S.; Tersoff, J.; Martel, R. V.; Derycke, V.; Appenzeller, J.; Avouris, Ph. *Phys. Rev. Lett.* **2002**, 89, 106801.
- (5) Freitag, M.; Radosavljevic, M.; Zhou, Y. X.; Johnson, A. T.; Smith, W. F. *Appl. Phys. Lett.* **2001**, 79, 3326.
- (6) Javey, A.; Guo, J.; Wang, Q.; Lundstrom, M.; Dai, H. *Nature* **2003**, 424, 654.
- (7) Martel, R.; Derycke, V.; Lavoie, C.; Appenzeller, J.; Chan, K. K.; Tersoff, J.; Avouris, Ph. *Phys. Rev. Lett.* **2001**, 87, 256805.
- (8) Balasubramanian, K.; Fan, Y.; Burghard, M.; Kern, K.; Wannek, U.; Mews, A. *Appl. Phys. Lett.* **2004**, 84, 2400.
- (9) Huang, L.; Cui, X.; White, B.; O’Brien, S. P. *J. Phys. Chem. B* **2004**, 108, 16451.

- (10) Huang, S.; Maynor, B.; Cai, X.; Liu, J. *Adv. Mater.* **2003**, *15*, 1651.
 Huang, S.; Cai, X.; Liu, J. *J. Am. Chem. Soc.* **2003**, *125*, 5636.
- (11) Freitag, M.; Martin, Y.; Misewich, J. A.; Martel, R.; Avouris, Ph. *Nano Lett.* **2003**, *3*, 1067.
- (12) Qiu, X.; Freitag, M.; Perebeinos, V.; Avouris, Ph. *Nano Lett.* **2005**, *5*, 749.
- (13) Split gates have been used to build CNT p–n junctions. These produce a photovoltage upon global illumination due to the built-in electric field at the junction. Refs: Lee, J. U.; Gipp, P. P.; Heller, C. M. *Appl. Phys. Lett.* **2004**, *85*, 145. Lee, J. U. *Appl. Phys. Lett.* **2005**, *87*, 073101.
- (14) Avouris, Ph.; Afzali, A.; Appenzeller, J.; Chen, J.; Freitag, M.; Klinke, C.; Lin, Y.-M.; Tsang, J. C. *Tech. Dig.—Int. Electron Devices Meet.* **2004**, 525–529.
- (15) Ahn, Y.; Dunning, J.; Park, J. *Nano Lett.* **2005**, *5*, 1367.
- (16) Balasubramanian, K.; Burghard, M.; Kern, K.; Scolari, M.; Mews, A. *Nano Lett.* **2005**, *5*, 507–510.
- (17) Freitag, M.; Tsang, J. C.; Avouris, Ph. To be submitted for publication.
- (18) Fuhrer, M. S.; Kim, B. M.; Durkop, T.; Brintlinger, T. *Nano Lett.* **2002**, *2*, 755–759.
- (19) Radosavljević, M.; Freitag, M.; Thadani, K. V.; Johnson, A. T. *Nano Lett.* **2002**, *2*, 761.
- (20) In the transistor on state, the open-circuit photovoltage from the nanotube bulk is reduced because the CNT is doped and recombination becomes more effective. The photovoltage from the Schottky barrier is further reduced because the depletion layer becomes very thin. Both effects also lead to diminishing short-circuit photocurrents at very high p-type doping. The fact that V_{OC} diminishes faster than I_{SC} is due to the increasing conductivity of the CNTFET for higher doping levels.
- (21) Cui, X.; Freitag, M.; Martel, R.; Brus, L.; Avouris, Ph. *Nano Lett.* **2003**, *3*, 783.
- (22) Cao, J.; Wang, Q.; Wang, D.; Dai, H. *Small* **2005**, *1*, 138.
- (23) Gu, Y.; Kwak, E.-S.; Lensch, J. L.; Allen, J. E.; Odom, T. W.; Lauthon, L. J. *Appl. Phys. Lett.* **2005**, *87*, 043111.
- (24) Murakami, Y.; Einarsson, E.; Edamura, T.; Maruyama, S. *Phys. Rev. Lett.* **2005**, *94*, 087402.

NL070900E